Masonry Confinement with Fiber-Reinforced Polymers

Theofanis D. Krevaikas[1] and Thanasis C. Triantafillou, M.ASCE[2]

Abstract: The application of fiber-reinforced polymer (FRP) as a means of increasing the axial capacity of masonry through confinement, a subject not addressed before, is investigated in this study. Four series of uniaxial compression tests, with a total of 42 specimens, were conducted on model masonry columns with these variables: number of layers, radius at the corners, cross-section aspect ratio, and type of fibers. It is concluded that, in general, FRP-confined masonry behaves very much like FRP-confined concrete. Confinement increases both the load-carrying capacity and the deformability of masonry almost linearly with the average confining stress. The uniaxial compression test results enabled the development of a simple confinement model for strength and ultimate strain of FRP-confined masonry. This model is consistent with the test results obtained here but should attract further experimental verification in the future to account for types of masonry materials other than those used in this study.

DOI: 10.1061/(ASCE)1090-0268(2005)9:2(128)

CE Database subject headings: Confinement; Fiber reinforced polymers; Masonry; Tests.

Introduction and Background

Masonry structures in need of intervention through strengthening constitute a significant portion of the building stock throughout the world, as either they have suffered from the accumulated effects of inadequate construction techniques and materials, seismic and wind loads, foundation settlements, and environmental deterioration, or they need to be upgraded to meet more stringent seismic design requirements, often combined with change in use.

In the past decade or so, traditional strengthening techniques for masonry (e.g., filling of cracks and voids by grouting, stitching of large cracks and other weak areas with metallic or brick elements or concrete zones, application of reinforced grouted perforations, external or internal posttensioning with steel ties, and single- or double-sided jacketing by shotcrete or by cast in situ concrete, in combination with steel reinforcement) have been supplemented with the fiber-reinforced polymer (FRP) strengthening technique, which involves epoxy bonding of strips or sheets, mainly in the direction of principal tensile stresses.

Studies on the use of FRP as a strengthening material for masonry have been numerous. Detailed concepts and analytical results on the applicability and effectiveness of FRP tendons used to apply circumferential prestressing to historic masonry structures were developed first by Triantafillou and Fardis (1993, 1997). A study on the use of epoxy-bonded carbon fiber-reinforced polymer (CFRP) strips as seismic strengthening elements of masonry was performed by Schwegler (1994), who demonstrated the effectiveness of this technique through full-scale in-plane and out-of-plane cyclic testing of one-story masonry walls and developed an analytical model for the in-plane behavior of CFRP-strengthened walls within the framework of stress fields theory. The work reported by Ehsani (1995) and Ehsani et al. (1997) focused on in-plane shear (monotonic static) testing of unreinforced masonry specimens strengthened with epoxy-bonded glass fabrics. A similar concept involving epoxy-bonded carbon overlays was studied by Laursen et al. (1995) and Seible (1995), who performed cyclic tests on approximately half-scale masonry wall panels and on a full-scale masonry building and proved that such overlays are highly effective in increasing the strength, reducing the shear deformations, and improving the overall structural ductility.

Detailed design equations and interaction diagrams for FRP-strengthened masonry under out-of-plane bending, in-plane shear, and in-plane bending, all combined with axial load, were developed by Triantafillou (1998). Experimental studies performed on masonry walls subjected to monotonic (Albert et al. 2001; Hamilton and Dolan 2001) and cyclic (Ehsani et al. 1999; Velazquez-Dimas and Ehsani 2000; Kuzik et al. 2003) out-of-plane loading, demonstrated the effectiveness of vertically placed glass fiber-reinforced polymer (GFRP) strips. The effectiveness of this system was also confirmed by Paquette et al. (2001) through shake table testing. Similar studies were conducted by Hamoush et al. (2001) on walls strengthened with overlays covering the full tensile zone, as well as with vertical and horizontal strips, and confirmed the effectiveness of the FRP systems as out-of-plane flexural strengthening elements. Tumialan et al. (2001) investigated the in-plane shear response of masonry walls strengthened with GFRP rods embedded into epoxy-based paste near the surface, at the locations of bed joints.

Recently the in-plane response of FRP-strengthened masonry has received a bit more attention than in past years: failure modes associated with in-plane response of masonry buildings and global response were analyzed by Moon et al. (2002) through push-over analysis; shake table testing of single masonry walls strengthened on one side with GFRP fabrics or vertical CFRP strips was performed by Badoux et al. (2002); cyclic loading of walls strengthened with vertical and horizontal GFRP or CFRP strips were conducted by Fam et al. (2002) and Marcari et al.

[1]PhD Candidate, Dept. of Civil Engineering, Univ. of Patras, Patras 26500, Greece.

[2]Associate Professor, Dept. of Civil Engineering, Univ. of Patras, Patras 26500, Greece. E-mail: ttriant@upatras.gr

Note. Discussion open until September 1, 2005. Separate discussions must be submitted for individual papers. To extend the closing date by one month, a written request must be filed with the ASCE Managing Editor. The manuscript for this paper was submitted for review and possible publication on March 4, 2004; approved on April 26, 2004. This paper is part of the ***Journal of Composites for Construction***, Vol. 9, No. 2, April 1, 2005. ©ASCE, ISSN 1090-0268/2005/2-128–135/$25.00.

(2003), supporting the effectiveness of this system; damage mechanisms of walls strengthened with CFRP strips under cyclic loading were studied by Gu et al. (2003); coupon-size masonry panels were tested in diagonal compression to simulate in-plane shear by Valuzzi et al. (2002) and Russo et al. (2003); and a strut-and-tie modeling methodology for the determination of optimum location and dimensioning of the FRP strips was developed by Krevaikas and Triantafillou (2005).

In another field of application, epoxy-bonded CFRP strips have been bonded to the extrados of vaults and arches, thus providing increased capacity against lateral loads [e.g., Borri et al. (2000); Faccio and Foraboschi (2000)]. The range of applicability of FRP has been extended to blast-loaded masonry by Muszynski and Purcell (2003), Patoary and Tan (2003), and Crawford and Morrill (2003), where it was proved that flexible, easy-to-apply glass, carbon, or (even better) hybrid glass/aramid fabrics offer interesting solutions.

The above survey of the literature reveals that the application of FRP as a means of increasing the axial capacity of masonry, for example, through confinement, has not been explored, except in Triantafillou and Fardis (1993, 1997), through the introduction of external prestressing, and Valuzzi et al. (2003), through the use of horizontally placed near-surface-mounted (in the bed joints) FRP strips. Despite the great potential of FRP-based confinement, which has received substantial attention in concrete structures, and despite the urgent need to develop effective methods of masonry confinement as a means of preventing catastrophic failures, for example, during earthquakes or even due to creep effects, no studies have been reported in this area, namely, masonry confinement through FRP wrapping. It is this gap that the writers intend to fill in this study, through both experimental and analytical developments.

Experimental Program

Test Specimens and Material Properties

A total of 42 model masonry column specimens in four series were prepared using clay bricks with dimensions of 55 mm (width), 40 mm (height), and 115 mm (length), bonded together with a mortar containing cement and lime as binder, at a water:cement:lime:sand ratio equal to 0.9:1:3:7.5 by weight. The cross-sectional area of the specimens was 115×115 mm (aspect ratio 1:1) in the first two series, 172.5×115 mm (aspect ratio 1.5:1) in the third, and 230×115 mm (aspect ratio 2:1) in the fourth. Each model column comprised bricks placed in seven rows with six bed joints in between, as shown in Fig. 1. The thickness of mortar was, in general, 10 mm, except in some of the head joints, where it was slightly reduced to maintain the desired cross-section aspect ratio. The corners of all specimens were rounded using a grinding machine at a radius of 10 mm in the first, third, and fourth series, and at a radius of 20 mm in the second series. Within each series, specimens were wrapped with one, two, or three layers of unidirectional CFRP sheets or with five layers of unidirectional GFRP sheets, applied through the use of a two-part epoxy adhesive.

Details about the model columns in each series are given in Table 1. In this table, each specimen type is given the notation FN_A_RX, where F = fiber type (C for carbon and G for glass); N = number of layers (1, 2, or 3 for carbon, 5 for glass); A = aspect ratio of cross-section dimensions (1 or 1.5 or 2), and X = radius at corners (10 or 20 mm). For instance, C2_1_R20 denotes specimens with square cross section (aspect ratio 1), corners rounded at 20 mm, and wrapping with two layers of carbon fabrics; G5_1.5_R10 denotes specimens with cross dimensions of aspect ratio 1.5, corners rounded at 10 mm, and wrapping with five layers of carbon fabrics. For specimens without wrapping (control), FN is denoted as Co. The number of identical specimens tested was either two or three (second column in Table 1).

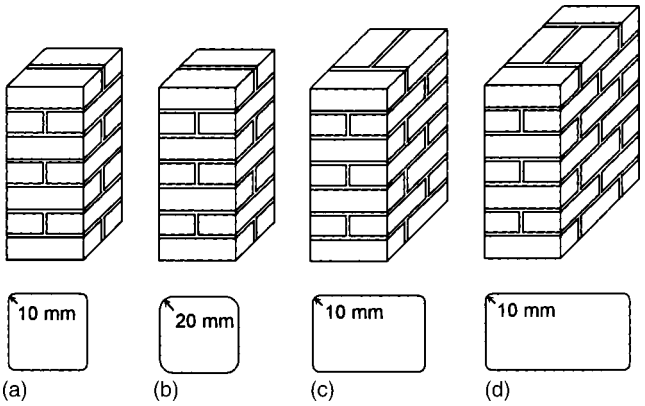

Fig. 1. Configuration of masonry walls tested: (a) square cross section, corner radius 10 mm; (b) square cross section, corner radius 20 mm; (c) cross section with aspect ratio 1.5:1, corner radius 10 mm; and (d) cross section with aspect ratio 2:1, corner radius 10 mm

The configurations described above allow investigation of the role of various parameters in the effectiveness of FRP jacketing as a means of confining masonry; these parameters include the aspect ratio of the cross section, the radius of rounding at the corners, the type of fibers, the number of layers, and the stiffness/strength characteristics of the jacket.

Before wrapping the FRP sheets, masonry surface defects were filled with epoxy putty. A layer of epoxy resin was next applied on the surface of each specimen, and then wrapping of the sheets was applied with the fibers in the hoop direction. After the wrapping of each lap of a fiber sheet, a layer of epoxy resin was applied and a roller used to remove air voids and allow better impregnation of the resin. The finishing end of the sheet overlapped the starting end by approximately 100 mm. Wrapping of the sheets took place after curing the specimens (actually the mortar) for at least one month in laboratory conditions, and testing started approximately one month after application of the FRP jackets.

The strength of the mortar was determined from compression testing of three $50 \times 50 \times 50$ mm cubes for each mortar mix; 28-day average strength results were as follows: 2.85, 2.15, 1.93, and 1.98 MPa in series 1, 2, 3, and 4, respectively. The bricks had an average compressive strength of 23.5 MPa, obtained through testing six 55-mm long orthogonal prisms (cut from bricks) of cross section 40×40 mm. Finally, the following properties (average values) were provided by the supplier of the fiber sheets: elastic modulus and tensile strength of CFRP jackets = 230 GPa and 3,500 MPa, respectively; and elastic modulus and tensile strength of GFRP jackets = 70 GPa and 2,000 MPa, respectively.

Experimental Setup and Procedure

The main objective of testing was to record the axial stress-strain curve and the failure mode of all the masonry specimens, which were subjected to axial loading applied monotonically under a

Table 1. Specimen Notation and Summary of Test Results

Specimen notation	Number of specimens	Compressive strength (f_{Mc}) (MPa)	Normalized strength (f_{Mc}/f_{Mo}) (−)	Ultimate strain (ε_{Muc}) (−)	Normalized confining stress (σ_{lu}/f_{Mo}) (−)
Series 1					
Co_1_R10	*3*	*12.07*	*1.000*	*0.0018*	*0.000*
C1_1_R10	3	13.63	1.129	0.0190	0.328
C2_1_R10	2	16.92	1.402	0.0223	0.656
C3_1_R10	3	25.42	2.106	0.0373	0.984
G5_1_R10	2	40.00	3.314	0.0644	1.484
Series 2					
C1_1_R20	2	16.87	1.398	0.0255	0.429
C2_1_R20	2	23.91	1.981	0.0375	0.858
C3_1_R20	2	34.69	2.874	0.0529	1.287
G5_1_R20	2	44.87	3.717	0.0623	1.941
Series 3					
Co_1.5_R10	*3*	*6.65*	*1.000*	*0.0045*	*0.000*
C2_1.5_R10	3	11.90	1.789	0.0093	0.833
C3_1.5_R10	3	17.29	2.600	0.0485	1.250
G5_1.5_R10	3	24.37	3.665	0.0690	1.885
Series 4					
Co_2_R10	*3*	*6.21*	*1.000*	*0.0044*	*0.000*
C2_2_R10	2	11.79	1.899	0.0102	0.579
C3_2_R10	2	12.00	1.932	0.0340	0.869
G5_2_R10	2	17.81	2.868	0.0604	1.310

displacement control mode in a compression testing machine of 1,200 kN capacity. Loads were measured using a load cell, and displacements were obtained using external linear variable differential transducers (LVDTs) mounted on the walls, at a gauge length of 200 mm in the middle part of each specimen.

Experimental Results and Discussion

Stress-Strain Behavior, Strength and Deformability, and Failure Modes

The stress-strain diagrams for series 1, 2, 3, and 4 are presented in Figs. 2–5, respectively. It can be observed that in all cases the diagrams are nearly bilinear, with a curved transition curve between the two linear parts; no descending branch was recorded. The first linear part of the diagrams is similar in most cases, whereas the second linear part depends very much on the cross-section aspect ratio, the corner radius, and the jacket characteristics, becoming steeper and longer as the number of layers or the radius at the corner increases. The average values of axial strength (peak stress in the stress-strain diagram) and ultimate strain in each series of identical specimens are given in the third and fifth columns, respectively, of Table 1.

The control specimens failed in a brittle manner by the formation of vertical cracks through the head joints and the bricks [Figs. 6(a and b)]. Despite the fact that material properties were quite similar, specimens with square cross sections (series 1 and 2) were stronger but failed at lower strain compared to those with a cross-section aspect ratio of 1.5 or 2 (series 3 and 4). The failure modes of FRP-wrapped specimens were identical in all cases. After their formation through mortar joints and bricks, vertical cracks became increasingly wide and the masonry between the cracks was crushed. This continued until the lateral expansion reached the capacity of FRP, which failed by fracture at the corners [Figs. 6(c and d)].

Discussion of Results

By examining the stress-strain curves and the results given in Table 1 in terms of strength and ultimate strain, the following observations can be made:

General: FRP jackets can significantly enhance both the strength and the deformability of masonry under axial load. Con-

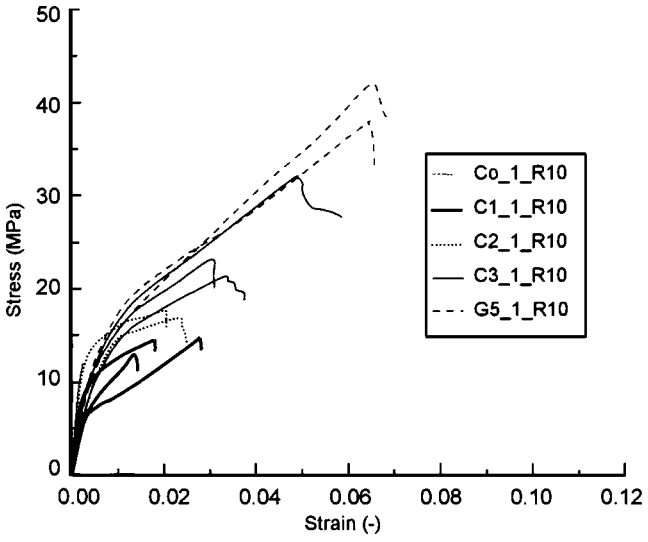

Fig. 2. Stress-strain curves for specimens in Series 1

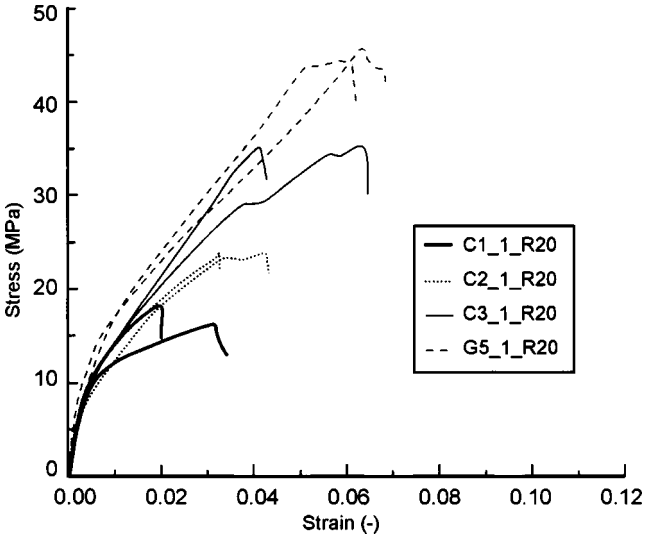

Fig. 3. Stress-strain curves for specimens in Series 2

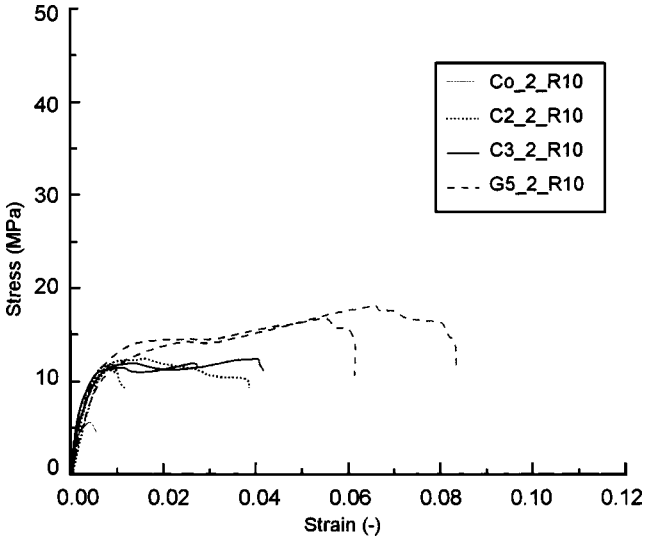

Fig. 5. Stress-strain curves for specimens in Series 4

finement effectiveness for strength, defined as the ratio of peak stress of FRP-confined masonry to that of the unconfined masonry, exceeded 3 (fourth column in Table 1). Enhancement in deformability was much more pronounced than gain in strength, as the ultimate strain of confined masonry exceeded that of unconfined masonry by a factor of more than 30.

Number of layers: In most cases, particularly when the cross-section aspect ratio was 1, strength and deformability increased almost linearly with the number of layers. In specimen Series 1, strength increased by about 13, 40, and 110%, and ultimate strain by a factor of 10, 12.5, and 20, for one, two, and three layers of CFRP. The respective increases in Series 2 were 40, 100, and 185% for strength and by a factor of 14, 21, and 29 for ultimate strain. In Series 3, strength increased by 80 and 160% and ultimate strain by a factor of 2 and 10 for two and three layers of CFRP. In Series 4, strength increased by about 90 and 95% and ultimate strain by a factor of 2.5 and 7.5 for two and three layers of CFRP, respectively.

Corner radius: When the corner radius was increased from 10 to 20 mm (Series 1 versus Series 2), the strength increased by about 25–40% with CFRP jackets and by about 12% with the very thick GFRP jackets. Hence the beneficial effect of increasing the corner radius was verified.

Aspect ratio: Due to the large difference in control specimen strength and ultimate strain values between series 1 and 3 or 4, a direct comparison of the results for all three aspect ratios is not possible. However, this comparison can be made between series 3 and 4, where it is observed that for all cases but one (when two layers of CFRP were used), the reduction in confinement effectiveness when the aspect ratio becomes 2 from 1.5 is about 20–25% for strength and about 10–20% for strain.

Type of fibers: As far as axial stiffness in the hoop direction is concerned, five layers of GFRP fall somewhere between two and three layers of CFRP. Yet the effectiveness of GFRP jackets with five layers was superior to that of CFRP, even compared with the three-layer CFRP jacket. This proves that the higher deformability of glass fibers, compared to carbon, makes them more effective as jacketing materials if comparisons are made for the same stiffness.

Overall, it may be argued that the response and failure of axially loaded masonry confined with FRP has many characteristics similar to those of concrete. Hence, the development of a confinement model could be based on existing knowledge of and experience with concrete. This model is attempted in the next section.

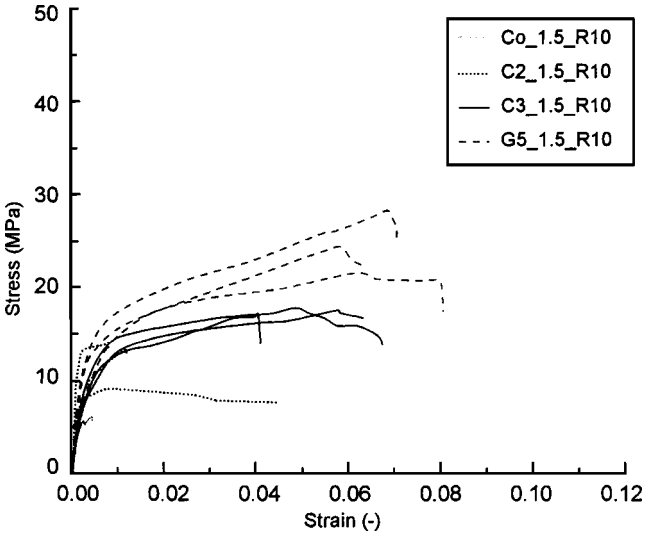

Fig. 4. Stress-strain curves for specimens in Series 3

Confinement Model

The basis of the FRP contribution to the strength and deformability of confined masonry is, by analogy to confined concrete, the transverse passive pressure σ_l developing in the masonry in response to the jacket forces. This pressure is, in general, nonuniform, especially near the corners of rectangular cross sections. As an average value for σ_l in a cross section with dimensions b and h, one may write (Fig. 7)

$$\sigma_l = \frac{\sigma_{l,h} + \sigma_{l,b}}{2} = \frac{1}{2} k_e \left(\frac{2t_f}{h} E_f \varepsilon_f + \frac{2t_f}{b} E_f \varepsilon_f \right) = k_e \frac{(b+h)}{bh} t_f E_f \varepsilon_f \tag{1}$$

where E_f=elastic modulus of FRP; ε_f=circumferential FRP strain; t_f=thickness of FRP; and k_e=effectiveness coefficient. For

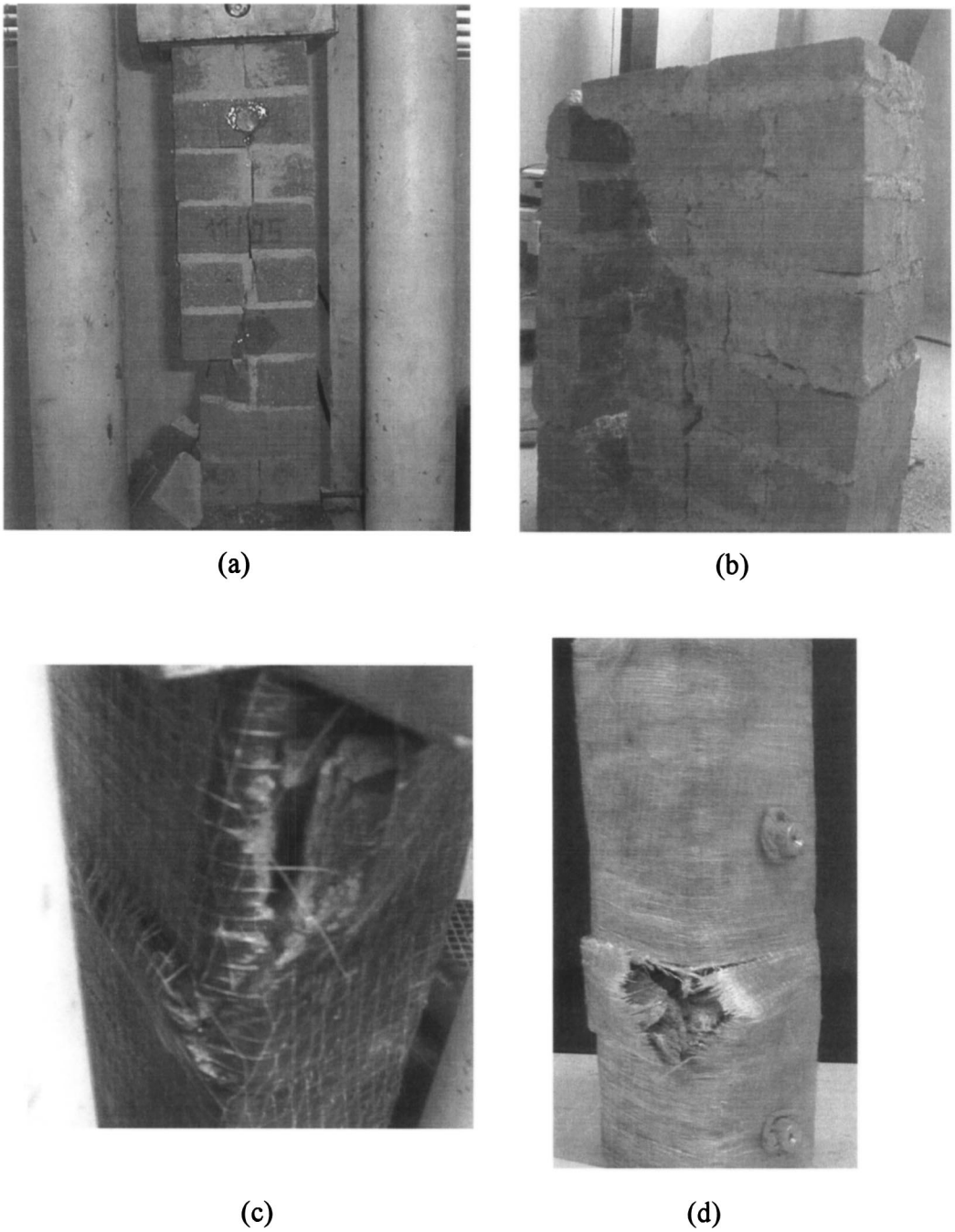

Fig. 6. Failure modes of unconfined and FRP-confined masonry: (a) vertical cracking in specimens with square cross section; (b) vertical cracking in specimens with cross section aspect ratio 2:1; (c) fracture of CFRP at corner; and (d) fracture of GFRP at corner

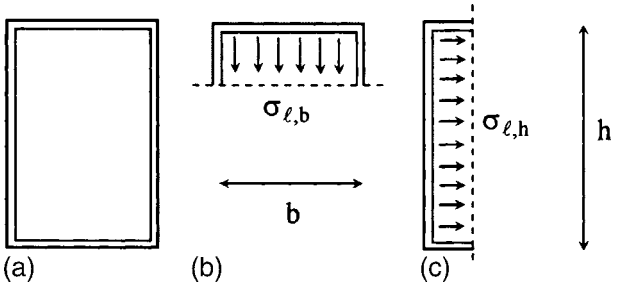

Fig. 7. Average confining stresses in rectangular cross sections

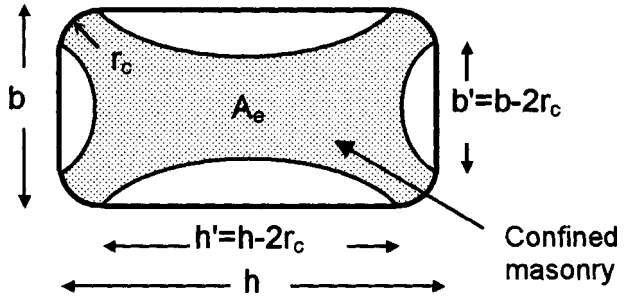

Fig. 8. Effectively confined masonry in columns with rectangular cross section

continuous FRP jackets with fibers in the direction perpendicular to the member axis, k_e is defined as the ratio of the effectively confined area (A_e in Fig. 8) to the total cross-sectional area A_g as follows [e.g., *fib* (2001)]:

$$k_e = 1 - \frac{b'^2 + h'^2}{3A_g} \tag{2}$$

Compressive failure of FRP-confined masonry occurs when the FRP jacket fractures at a hoop stress equal to the hoop tensile strength, f_{fe}, which is in general less than the uniaxial tensile strength of FRP (due to the multiaxial state of stress, stress concentrations, etc.). Hence the confining stress at failure, σ_{lu}, is given by Eq. (1) with $E_f\varepsilon_f$ replaced by f_{fe}:

$$\sigma_{lu} = k_e \frac{(b+h)}{bh} t_f f_{fe} \tag{3}$$

The model proposed here for FRP-confined masonry is based on the well-known form of models typically adopted for FRP-confined concrete [see, for instance, De Lorenzis and Tepfers (2003) for a comparative study of confinement models]:

$$f_{Mc} = f_{Mo}\left(1 + k_1 \frac{\sigma_{lu}}{f_{Mo}}\right) \tag{4}$$

$$\varepsilon_{Muc} = \varepsilon_{Muo} + k_2 \frac{\sigma_{lu}}{f_{Mo}} \tag{5}$$

where f_{Mc}=compressive strength of confined masonry; f_{Mo} =compressive strength of unconfined masonry; ε_{Muc}=ultimate strain of confined masonry; ε_{Muo}=ultimate strain of unconfined masonry; and k_1, k_2=empirical constants. Experimental evidence both for concrete and for masonry confined with low volumetric fractions of transverse (confining) reinforcement suggests that for very low values of the confining stress the confined compressive strength does not exceed the unconfined value. Hence, Eq. (4) can be rewritten as follows:

$$f_{Mc} = f_{Mo}\left(\alpha + k_1 \frac{\sigma_{lu}}{f_{Mo}}\right) \leqslant f_{Mo} \tag{6}$$

with $\alpha < 1$ to ensure continuity of f_{Mc} at the level of confining stress beyond which $f_{Mc} \geqslant f_{Mo}$.

The aforementioned confinement model for masonry is defined fully by determining the empirical constants k_1, k_2 and α from testing. Test data obtained in this study for the ratio of confined to unconfined strength, f_{Mc}/f_{Mo}, in terms of the normalized confining stress, σ_{lu}/f_{Mo} (see last column in Table 1) are plotted in Fig. 9. The best-fit linear equation to these data resulted in $\alpha = 0.6$ and $k_1 = 1.65$. Substituting these values in Eq. (6) and taking $f_{Mc}/f_{Mo} = 1$, the ratio σ_{lu}/f_{Mo} becomes equal to 0.24. Hence the proposed model for strength, shown by the solid lines in Fig. 9, is written as follows:

$$f_{Mc} = f_{Mo} \quad \text{if } \frac{\sigma_{lu}}{f_{Mo}} \leqslant 0.24 \tag{7a}$$

$$f_{Mc} = f_{Mo}\left(0.6 + 1.65 \frac{\sigma_{lu}}{f_{Mo}}\right) \quad \text{if } \frac{\sigma_{lu}}{f_{Mo}} \geqslant 0.24 \tag{7b}$$

The experimental data for the ultimate axial strain of confined masonry, ε_{Muc}, in terms of σ_{lu}/f_{Mo}, are plotted in Fig. 10. Again, the best-fit linear equation to these data was obtained as follows:

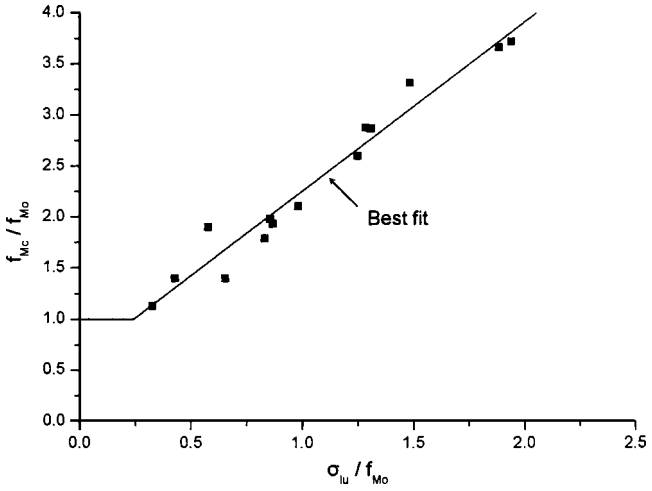

Fig. 9. Normalized compressive strength of confined masonry in terms of lateral confinement

$$\varepsilon_{Muc} = 0.005 + 0.034 \frac{\sigma_{lu}}{f_{Mo}} \tag{8}$$

Hence k_2 in Eq. (5) may be taken equal to 0.034, so that the proposed model for ultimate strain is as follows:

$$\varepsilon_{Muc} = \varepsilon_{Muo} + 0.034 \frac{\sigma_{lu}}{f_{Mo}} \tag{9}$$

Note that the line plot of Eq. (9) maintains the slope of the best fit (solid line in Fig. 10) but is shifted slightly downward, so that the intersection with the vertical axis becomes equal to the unconfined strain ε_{Muo} (dashed line in Fig. 10).

Conclusions

Confinement of masonry with FRP has not been investigated in the past. This study presents an experimental investigation on the behavior of axially loaded short masonry columns confined with FRP jackets, followed by the development of an analytical model for the prediction of confined strength and ultimate strain. Four

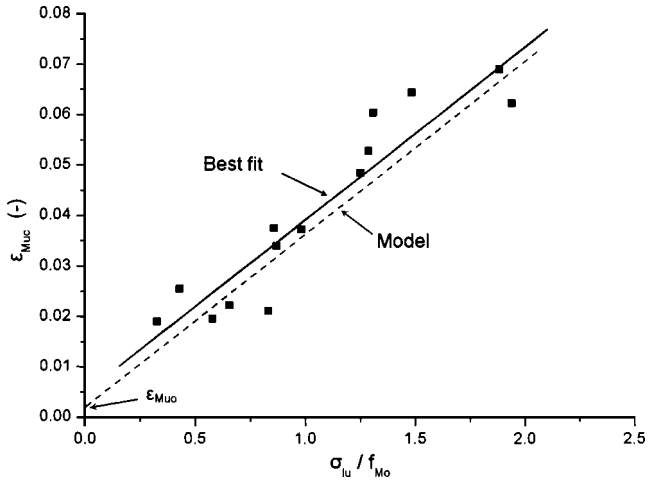

Fig. 10. Ultimate compressive strain of confined masonry in terms of lateral confinement

series of uniaxial compression tests, a total of 42 specimens, were conducted on specimens with these variables: number of layers, radius at the corners, cross-section aspect ratio, and type of fibers. The results are summarized as follows:

1. In general, FRP-confined masonry behaves very much like FRP-confined concrete. The confinement provided by FRP improves considerably both the load-carrying capacity and the deformability of masonry columns of rectangular cross section.
2. For the specimens tested in this study, the gain in performance (strength and deformability) increases almost linearly with the average confining stress. Increasing the corner radius or decreasing the cross-section aspect ratio is beneficial to the strength and strain capacity of rectangular masonry columns. Being more deformable, glass fibers are more effective than carbon fibers if the gain in strength and deformability is compared for the same FRP hoop stiffness.
3. Test results enabled the development of a simple confinement model for strength and ultimate strain of FRP-confined masonry. This model is consistent with test results obtained here, but should attract further experimental verification in the future to account for types of masonry materials other than those used in this study.

Acknowledgments

Eleftherios Tentolouris provided valuable assistance during preparation and testing of some of the specimens. SINTECNO provided the composite materials free of charge.

Notation

The following symbols are used in this paper:

A_e = effectively confined area;
A_g = gross section area;
b = cross-section width;
E_f = elastic modulus of FRP;
f_{fe} = effective tensile strength of FRP in hoop direction;
f_{Mc} = compressive strength of confined masonry;
f_{Mo} = compressive strength of unconfined masonry;
h = cross-section height;
k_e = confinement effectiveness coefficient;
k_1, k_2 = empirical constants;
t_f = thickness of FRP jacket;
α = empirical constant;
ε_f = strain in FRP jacket;
ε_{Muc} = ultimate strain of confined masonry;
ε_{Muo} = ultimate strain of unconfined masonry;
σ_l = lateral stress due to FRP wrapping;
$\sigma_{l,b}$ = lateral stress perpendicular to side b;
$\sigma_{l,h}$ = lateral stress perpendicular to side h; and
σ_{lu} = ultimate lateral stress due to FRP wrapping.

References

Albert, M. L., Elwi, A. E., and Cheng, J. J. R. (2001). "Strengthening of unreinforced masonry walls using FRPs." *J. Compos. Constr.*, 5(2), 76–84.

Badoux, M., Elgwady, M. A., and Lestuzzi, P. (2002). "Earthquake simulator tests on unreinforced masonry walls before and after upgrading with composites." *12th European Conf. on Earthquake Engineering*, Elsevier Science, London.

Borri, A., Avorio, A., and Bottardi, M. (2000). "Theoretical analysis and a case study of historical masonry vaults strengthened by using advanced FRP." *Advanced composite materials in bridges and structures III*, J. Humar and A. G. Razaqpur, eds., Canadian Society for Civil Engineering, Montréal, 577–584.

Crawford, J. E., and Morrill, K. B. (2003). "Retrofit techniques using polymers and FRPs for preventing injurious wall debris." *6th Int. Conf. on Fibre-Reinforced Plastics for Reinforced Concrete Structures*, K. H. Tan, ed., World Scientific, Singapore, 1199–1208.

De Lorenzis, L., and Tepfers, R. (2003). "Comparative study of models on confinement of concrete cylinders with fiber-reinforced polymer composites." *J. Compos. Constr.*, 7(3), 219–237.

Ehsani, M. R. (1995). "Strengthening of earthquake-damaged masonry structures with composite materials." *Non-metallic (FRP) reinforcement for concrete structures*, L. Taerwe, ed., E&FN Spon, London, 680–687.

Ehsani, M. R., Saadatmanesh, H., and Al-Saidy, A. (1997). "Shear behavior of URM retrofitted with FRP overlays." *J. Compos. Constr.*, 1(1), 17–25.

Ehsani, M. R., Saadatmanesh, H., and Velazquez-Dimas, J. I. (1999). "Behavior of retrofitted URM walls under simulated earthquake loading." *J. Compos. Constr.*, 3(3), 134–142.

Faccio, P., and Foraboschi, P. (2000). "Experimental and theoretical analysis of masonry vaults with FRP reinforcements." *Advanced composite materials in bridges and structures III*, J. Humar and A. G. Razaqpur, eds., Canadian Society for Civil Engineering, Montréal, 629–636.

Fam, A., Musiker, D., Kowalsky, M., and Rizkalla, S. (2002). "In-plane testing of damaged masonry wall repaired with FRP." *Advanced Composite Letters*, 11(6), 277–283.

fib. (2001). "Externally bonded FRP reinforcement for RC structures." *Bulletin 14*, International Federation for Structural Concrete, Lausanne, Switzerland.

Gu, X. L., Ouyang, Y., Zhang, W. P., and Ye, F. F. (2003). "Seismic behaviour of masonry structural walls strengthened with CFRP plates." *6th Int. Conf. on Fibre-Reinforced Plastics for Reinforced Concrete Structures*, K. H. Tan, ed., World Scientific, Singapore, 1259–1268.

Hamilton III, H. R., and Dolan, C. W. (2001). "Flexural capacity of glass FRP strengthened concrete masonry walls." *J. Compos. Constr.*, 5(3), 170–178.

Hamoush, S. A., McGinley, M. W., Mlakar, P., Scott, D., and Murray, K. (2001). "Out-of-plane strengthening of masonry walls with reinforced composites." *J. Compos. Constr.*, 5(3), 139–145.

Krevaikas, T. D., and Triantafillou, T. C. (2005). "Computer-aided strengthening of masonry walls using fibre-reinforced polymer strips." *Mater. Struct.* (in press).

Kuzik, M. D., Elwi, A. E., and Cheng, J. J. R. (2003). "Cyclic flexure tests of masonry walls reinforced with glass fiber reinforced polymer sheets." *J. Compos. Constr.*, 7(1), 20–30.

Laursen, P. T., Seible, F., Hegemier, G. A., and Innamorato, D. (1995). "Seismic retrofit and repair of masonry walls with carbon overlays." *Non-metallic (FRP) reinforcement for concrete structures*, L. Taerwe, ed., E&FN Spon, London, 617–623.

Marcari, G., Manfredi, G., and Pecce, M. (2003). "Experimental behaviour of masonry panels strengthened with FRP sheets." *6th Int. Conf. on Fibre-Reinforced Plastics for Reinforced Concrete Structures*, K. H. Tan, ed., World Scientific, Singapore, 1209–1218.

Moon, F. L., Yi, T., Leon, R. T., and Kahn, L. F. (2002). "Seismic strengthening of unreinforced masonry structures with FRP overlays and post-tensioning." *12th European Conf. on Earthquake Engineering*, Elsevier Science, London.

Muszynski, L. C., and Purcell, M. R. (2003). "Use of composite reinforcement to strengthen concrete and air-entrained concrete masonry walls against air blast." *J. Compos. Constr.*, 7(2), 98–108.

Paquette, J., Bruneau, M., and Filiatrault, A. (2001). "Out-of-plane seismic evaluation and retrofit of turn-of-the-century North American masonry walls." *J. Struct. Eng.*, 127(5), 561–569.

Patoary, M. K. H., and Tan, K. H. (2003). "Blast resistance of prototype in-built masonry walls strengthened with FRP systems." *6th Int. Conf. on Fibre-Reinforced Plastics for Reinforced Concrete Structures*, K. H. Tan, ed., World Scientific, Singapore, 1189–1198.

Russo, S., Gottardo, R., and Codato, D. (2003). "Effect of FRP mesh reinforcement on shear capacity and deformability of masonry walls." *6th Int. Conf. on Fibre-Reinforced Plastics for Reinforced Concrete Structures*, K. H. Tan, ed., World Scientific, Singapore, 1239–1248.

Schwegler, G. (1994). "Masonry construction strengthened with fiber composites in seismically endangered zones." *10th European Conf. on Earthquake Engineering*, Balkema, Rotterdam, The Netherlands, 454–458.

Seible, F. (1995). "Repair and seismic retest of a full-scale reinforced masonry building." *6th Int. Conf. on Structural Faults and Repair*, Vol. 3, 229–236.

Triantafillou, T. C. (1998). "Strengthening of masonry structures using epoxy-bonded FRP laminates." *J. Compos. Constr.*, 2(2), 96–104.

Triantafillou, T. C., and Fardis, M. N. (1993). "Advanced composites as strengthening materials of historic structures." *IABSE Symp. on Structural Preservation of the Architectural Heritage*, International Association for Bridge and Structural Engineering, Lisbon, Portugal, 541–548.

Triantafillou, T. C., and Fardis, M. N. (1997). "Strengthening of historic masonry structures with composite materials." *Mater. Struct.*, 30, 486–486.

Tumialan, G., Huang, P.-C., Nanni, A., and Silva, P. (2001). "Strengthening of masonry walls by FRP structural repointing." *5th Int. Conf. on Fibre-Reinforced Plastics for Reinforced Concrete Structures*, C. J. Burgoyne, ed., Thomas Telford, Cambridge, U.K., 1033–1042.

Valuzzi, M. R., Tinazzi, D., and Modena, C. (2002). "Shear behavior of masonry panels strengthened by FRP laminates." *Constr. Build. Mater.*, 16, 409–416.

Valuzzi, M. R., Tinazzi, D., and Modena, C. (2003). "Strengthening of masonry structures under compressive loads by using FRP strips" *6th Int. Conf. on Fibre-Reinforced Plastics for Reinforced Concrete Structures*, K. H. Tan ed., World Scientific, Singapore, 1249–1258.

Velazquez-Dimas, J. I., and Ehsani, M. R. (2000). "Modeling out-of-plane behavior of URM walls retrofitted with fiber composites." *J. Compos. Constr.*, 4(4), 172–181.